MolecularMedicine

Excessive Reversal of Epidermal Growth Factor Receptor and Ephrin Signaling Following Tracheal Occlusion in Rabbit Model of Congenital Diaphragmatic Hernia

Brian M Varisco,[1] Lourenco Sbragia,[2,3] Jing Chen,[4] Federico Scorletti,[2,3] Rashika Joshi,[1] Hector R Wong,[1] Rebeca Lopes-Figueira,[2,3] Marc Oria,[2,3] and Jose Peiro[2,3]

[1]Cincinnati Children's Hospital Medical Center (CCHMC) Division of Critical Care Medicine; [2]CCHMC Division of Pediatric General and Thoracic Surgery; [3]The Center for Fetal, Cellular, and Molecular Therapy (CCHMC); and [4]CCHMC Division of Biomedical Informatics, Cincinnati, Ohio, United States of America

Congenital diaphragmatic hernia (CDH) causes severe pulmonary hypoplasia from herniation of abdominal contents into the thorax. Tracheal occlusion (TO) for human CDH improves survival, but morbidity and mortality remain high, and we do not fully understand the cellular pathways and processes most severely impacted by CDH and TO. We created a left diaphragmatic hernia (DH) in rabbit fetuses with subsequent TO and collected left lung sections for NextGen mRNA sequencing. DH, TO and DHTO fetuses had comparable body and organ growth to control except for lower lung weights in DH ($p < 0.05$). Of 13,687 expressed genes, DHTO had 687 differentially expressed genes compared with DH, but no other group-group comparison had more than 10. Considering genes in combination, many of the genes reduced in DH were more highly expressed in DHTO than in control. Benchmarking fetal rabbit lung gene expression to published lung development data, both DH and DHTO lungs were more highly correlated with the gene expression of immature lung. DNA synthesis was upregulated in DHTO compared with DH and ribosome and protein synthesis pathways were downregulated. DH reduced total and epithelial cell proliferation by half and two-thirds respectively, and DHTO increased proliferation by 2.5 and 3.4-fold respectively. Signaling pathways downregulated by DH and upregulated in DHTO were epidermal growth factor receptor signaling, ephrin signaling and cell migration; however, levels of ephrin and EGFR signaling in DHTO exceeded that of control. Identification and inhibition of the ligands responsible for this dysregulated signaling could improve lung development in CDH.

Online address: http://www.molmed.org
doi: 10.2119/molmed.2016.00121

INTRODUCTION

Congenital diaphragmatic hernia (CDH) occurs in approximately 1 in 3,000 births with half of these defects being severe and the majority involving the left diaphragm (1). In CDH, the pleuroperitoneal folds fail to fuse with the central tendon during the eighth week of gestation permitting herniation of abdominal contents into the thorax resulting in severe pulmonary hypoplasia (2). Despite optimal medical and surgical care, mortality remains high with survivors experiencing severe restrictive lung disease and significant pulmonary hypertension (1).

A logical intervention for CDH is to expand the lungs *in utero*. Since the lung epithelium secretes fluid into the future airspace, fetal tracheal occlusion (TO) results in lung distention (3). The first reports of TO for human CDH suggested improved survival and outcomes (4). TO for CDH in humans is typically placed at the 28th week of gestation and removed during the 34th week. A meta-analysis of over 200 human fetuses treated with this approach demonstrated decreased mortality (5). While TO for CDH may gain more widespread acceptance in the coming years, there remains an urgent need to understand the cellular responses to CDH and TO so that targeted therapies may be developed to improve fetal lung development and to limit any undesirable effects of TO. There have been reports of how CDH and TO impact lung matrix synthesis (6–9), lung epithelial function and surfactant (10–13) and microvascular development (14–16), and that tracheal occlusion reverses some of

Address correspondence to *Brian Varisco, Cincinnati Children's Hospital Medical Center, Division of Critical Care Medicine, 3333 Burnet Avenue, MLC 2005, Cincinnati, OH, 45229. Phone: 513-636-4259; Fax: 513-636-4267; E-mail: brian.varisco@cchmc.org.*
Submitted May 4, 2016; Accepted for publication July 11, 2016; Published Online (www.molmed.org) July 19, 2016.

Feinstein Institute for Medical Research
Northwell Health™

the gene expression changes induced by diaphragmatic hernia (17). However, we used a bioinformatics approach to understand what cellular processes are dysregulated in CDH and how they are changed in CDHTO.

Using a fetal rabbit surgical model of CDH with TO, we created a left diaphragmatic hernia (DH) in rabbit fetuses at a time period corresponding to late pseudoglandular stage of lung development, performed TO at the beginning of the canalicular stage of lung development, and collected lungs for Next Generation sequencing just before birth which in the rabbit is at the beginning of the alveolar stage of lung development. By benchmarking lung gene expression to published mouse lung development gene expression profiles, we hypothesized that DH would maintain the fetal lung in a more immature state which would be reversed by TO. We furthermore hypothesized that the pathways and processes impacted by DH would be partially reversed by TO, and processes regulated by cyclic versus tonic stretch could be defined by comparing gene expression profiles of TO and DHTO lungs.

MATERIALS AND METHODS

Animal Care and Use

Animal use was approved by The *Cincinnati Children's Hospital Institutional Animal Care and Use Committee*. Timed pregnant New Zealand Rabbits were maintained at 24°C with 12 h light/dark cycles for 2 wks and received rabbit specific chow and water *ad libitum* until the moment of surgery.

Experimental Groups

The fetuses of nine pregnant rabbits were divided in 4 experimental groups (n = 6 per group). 1) Control: Rabbit fetuses at 30.5 d of gestation (E30.5) not directly operated upon; 2) DH: left diaphragmatic hernia at E25; 3) TO: tracheal occlusion at E27 and 4) DHTO: DH surgery at E25 and TO surgery at E27. All rabbit fetus groups were sacrificed at E30.5. After fetal harvest, the pregnant rabbit was euthanized. Postnatal day one (P1) kits were euthanized 24 h after birth as a comparison group.

Surgical Procedures

Surgical preoperatory. Pregnant rabbits were weighed and anesthetized with ketamine (35 mg/kg) (Parke-Davis) and xylazine (5 mg/kg) (Butler Animal Health) and endotracheally intubated titrating isoflurane (Piramal Critical Care Inc.) to maintain anesthesia. If the pregnant rabbit was spontaneously breathing, then it was provided 1 liter per minute humidified oxygen and 2%–2.5% isoflurane through a T-piece. If the rabbit was not spontaneously breathing, it was placed on a ventilator with the same gas mixture. After shaving the surgical site was cleaned with 2% chlorhexidine alternating with 70% isopropyl alcohol 70% iodide three times.

Monitoring. Body temperature was maintained at 37°C with a heated water blanket and warmed normal saline solution with 5% dextrose was administered at a rate of 4 mL/kg/hr. Oxygen saturation, heart rate, transcutaneous CO_2 and core body temperature were monitored.

Hysterotomy. E25 and E27 (term = 31 d) pregnant rabbits were subjected to surgery under aseptic conditions. A median laparotomy was created, and one of the uterine horns was exposed. The fetuses were identified by numbers from the ovaries to the cervix with the fetus closest to the ovaries identified as fetus number 1, and the surgical procedure for creation of a left diaphragmatic hernia (DH) was performed on the fetus 1 and 2 for each horn. Tracheal occlusion was performed on fetuses 1 and 3 with fetus 4 being used as control.

Surgical creation of DH. The procedure was performed as described by Fauza, *et al*. at 25 d of gestation (18). An incision on the uterine wall was made and the fetus was exposed. A left posterior thoracotomy was performed, and the diaphragm muscle was identified and gently cut with micro-scissors until abdominal contents were observed coming up to the thorax. Then the thorax and hysterotomy sites were closed and 2 mL of warm normal saline solution was infused into the amniotic cavity. Fetuses in the other uterine horn were similarly operated upon. The abdominal wall was closed in two planes.

Tracheal occlusion. TO was performed according Debeer, *et al*. (15). On d 27 the uterus was opened and the fetal head and neck were exposed. The trachea was exposed using a midline incision and the trachea was ligated with a 4.0 Vicryl. The head was returned to the uterus and uterine and skin closure was completed as in the DH surgery.

Fetal tissue harvest. At E30.5, pregnant rabbits and fetuses were anesthetized with visual confirmation of DH and TO surgeries. Each fetus was removed from the uterus and weighed with organ collection and measurement per experimental needs. After fetal harvest, the pregnant rabbit was euthanized using thioembutal and potassium chloride intravenously.

Post Operatory Care

For survival surgeries, after recovery from anesthesia, one hundred mL of warm normal saline was administered subcutaneously (for slower absorption than intravenous fluids). Medroxyprogesterone acetate (4.5 mg/kg, Pfizer Inc.) was administered intramuscularly to prevent abortion. Enrofloxacin (5 mg/kg) (Bayer HealthCare LLC, Animal Health Division) and carprofen (2 mg/kg) (Zoetis) were administered subcutaneously. Carprofen was administered daily for 3 d post op, and enrofloxacin was administered twice daily for 5 d post op.

Morphological Assessment

To evaluate the effect of CDH on lung and somatic growth and development, we measured the body, heart, liver and bilateral lung weights of rabbit fetuses and pups.

Lung RNA Isolation and Quality Assessment

Lung tissues were stored at –80°C. The lateral aspect of the left upper lobe (approximately 10 mg of tissue) was

homogenized in RLT buffer from the RNEasy Mini kit (Qiagen) using a 4.5 mm Tissue Tearor Homogenizer (Cole-Parmer). After DNase treatment (30 units, PureLink DNASE Kit, ThermoFisher) RNA was isolated using the RNEasy Mini kit per manufacturer protocol. After elution in 50 μL of molecular grade water, RNA quality was analyzed using an Agilent 2100 Expert Bioanalyzer (Agilent Technologies). The three samples from each group with the highest RNA quality were used for sequencing.

Lung mRNA Sequencing

A cDNA library was created and sequenced using an IlluminaHiSeq2500 (Illumina) with 20 million paired-end reads per sample.

RNA-seq Data Analysis

Normalized RNA-seq gene counts of expressed genes were analyzed by Spearman's correlation with exclusion of samples with coefficients < 0.95. Differential gene expression analysis was performed using linear models based on log2-transformed gene counts and associated precision weights using limma (19). The precision weights were estimated using the variance modeling at the observational level (voom) (20). Specifically, a linear model was fitted for every gene with experiment conditions as the independent variables, and the desired comparisons were made by estimating the corresponding contrasts. The differential expression analysis estimated the gene expression changes (log-fold change) and their statistical significances (p value) for each comparison. False discovery rate (FDR) adjusted p values were also estimated. Genes with FDR adjusted p value < 0.1 were considered as statistically significantly differentially expressed genes. Functional genomic analysis was based on human genome annotations, with gene mappings from rabbit to human using Augmented Annotation and Orthologue Analysis for *Oryctolagus cuniculus* (21). Significant Gene Ontology categories and KEGG pathways were identified based on functional enrichment analysis of differentially expressed genes (22). Hierarchical clustering analysis was used to cluster samples and genes, with 1- correlation coefficient as distance measure and average agglomeration. RNA-seq analysis was performed using R statistical computing platform with KEGG plots created using pathview package (23).

Gene Expression Dynamics Inspector

A list of genes expressed in both our fetal rabbit lung data set and a mouse lung development data set (24) was generated. The fetal rabbit lung data set was used to create a two dimensional gene expression matrix using the publicly available GEDI platform (25). Mouse development lung gene expression was scaled to normalize median gene expression and then overlaid on this same matrix (that is, the same genes were in the same locations of the matrix).

Comparison to Published Datasets

We compared gene expression results in our dataset with a recently published one in the same fetal rabbit surgical model (17) by categorizing upregulated or downregulated genes in a contingency table and comparing them by Fisher's exact test.

Mouse Lung Development Benchmarking

Mean gene expression for each group was compared with two previously published data sets of whole lung gene expression over the course of lung development (24,26). Gene mapping from mouse to human was based on MGD Vertebrate Homology table (27). Spearman correlation coefficients were calculated at each developmental time point for each experimental group and plotted as correlation versus developmental age.

Lung Section Staining and Imaging

The left lower lobe was snap frozen, embedded in OCT (Sakura) and maintained at –80°C. Ten micron sections were mounted and stained with antiphospho-histone-3 (pH3, 1:200 Santa Cruz Biotechnology), and antithyroid transcription factor 1 (TTF1, Nkx2.1, 1:200, generous gift of Jeffrey Whitsett) with appropriate fluorophore-conjugated secondary antibodies. After secondary antibody incubation, sections were counterstained with CF405S hydrazide 1ng/mL (Biotium) and TO-PRO-3 Iodide (1 nmol/L, Life Technologies) with subsequent washes and mounting in Prolong Gold (Life Technologies). Tiled 4 × images were obtained on a Nikon Ti-E SpectraX widefield microscope with AndroZyla 4.2 SCMOS camera with 4-channel LED illumination. Nikon Elements software was used for quantative image by thresholding the nuclear, TTF-1 and pH3 signals based on negative control and counting the number of nuclei, pH3-positive nuclei, and pH3 and TTF-1 double positive nuclei. Confocal images were obtained on a Nikon A1 LUNV inverted confocal microscope with GaAsp detection unit. These images were not quantified.

PCR

Residual RNA from NextGen sequencing was to make cDNA with quantification of 18S and GAPDH RNA using proprietary primers from Applied Biosystems.

Statistical Analysis

For gross measurements, statistical comparison were performed with one way ANOVA and Tukey *post-test* for morphological analysis using GraphPad Instat 3.00 (GraphPad PRism software). Tests were two-tailed, and values of $p < 0.05$ were be considered significant. Error bars represent standard error of the mean.

RESULTS

Fetal Rabbit CDH Model

Fetal rabbit and fetal human lung development are comparable (28), and surgical creation of a diaphragmatic hernia during the pseudoglandular stage of lung development (E25) induces changes comparable to those seen in human

CDH (29). Tracheal occlusion (TO) was performed at E27 corresponding to the beginning of the canalicular stage. Lungs were collected for analysis at E30.5 corresponding to the beginning of the alveolar stage of lung development. The timing of TO and lung collection roughly correspond to the stages of development at which TO is placed and removed in human fetuses respectively (Figure 1) (30). Left diaphragmatic hernia (Figure 2A,B) permitted herniation of abdominal contents into the thorax, displaced thoracic organs to the right, and caused lung hypoplasia (Figure 2C,D). TO after DH increased lung size, restored spatial relationships and reduced herniation of abdominal contents (Figure 2E). TO alone caused lung hyperplasia (Figure 2F). This fetal rabbit surgical model faithfully models many clinical features of human CDH with TO.

Fetal Growth and Lung Size in the Fetal Rabbit DH Model

We measured lung and fetal/pup growth parameters to assess the impact of DH and TO on fetal well-being. There was no difference in rabbit fetal weights in control, DH, TO, or DHTO groups. P1 pup weights, heart weights and liver weights were greater than fetal weights, but there was no difference between nonlung fetal measurements (Figure 3A–C). DH reduced both right and left lung weights compared with all other groups, and this decrease was reversed by tracheal occlusion. Tracheal occlusion in the absence of DH increased the left lung beyond that of control (Figure 3D,F). These data demonstrate that the DH and TO surgeries induce bilateral lung hypoplasia but do not adversely impact other aspects of fetal growth.

Left Lung RNA Quality Assessment

We collected RNA from the left lower lobes of fetuses and pups and performed mRNA sequencing on samples from different mothers. In assessing the quality of these samples and performing principal component analysis, all had RNA integrity numbers of 9.4 or greater, but upon principal component analysis, two samples demonstrated a high degree of heterogeneity compared with the others. These two samples (one TO, one DH) were excluded from further analysis giving three P1, three control, two DH, two TO and three DHTO samples used in analysis. There were no gross morphological differences in these lungs at the time of collection. Only genes with one or more count per million in at least three samples were used for analysis (13,687 genes).

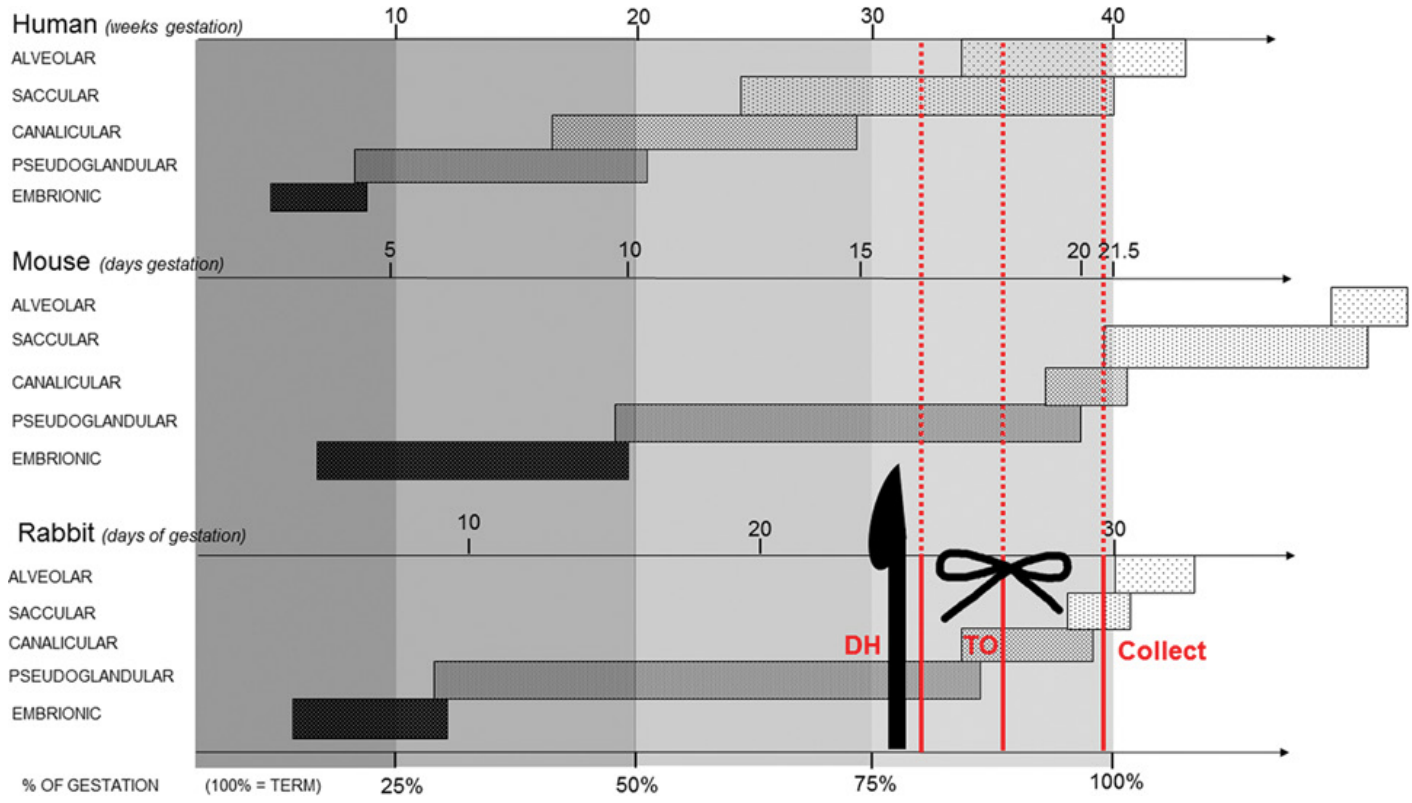

Figure 1. CDH and CDH/TO Model Overview. Comparison of human, rabbit and mouse lung development and with time points of each intervention in the fetal rabbit model (30).

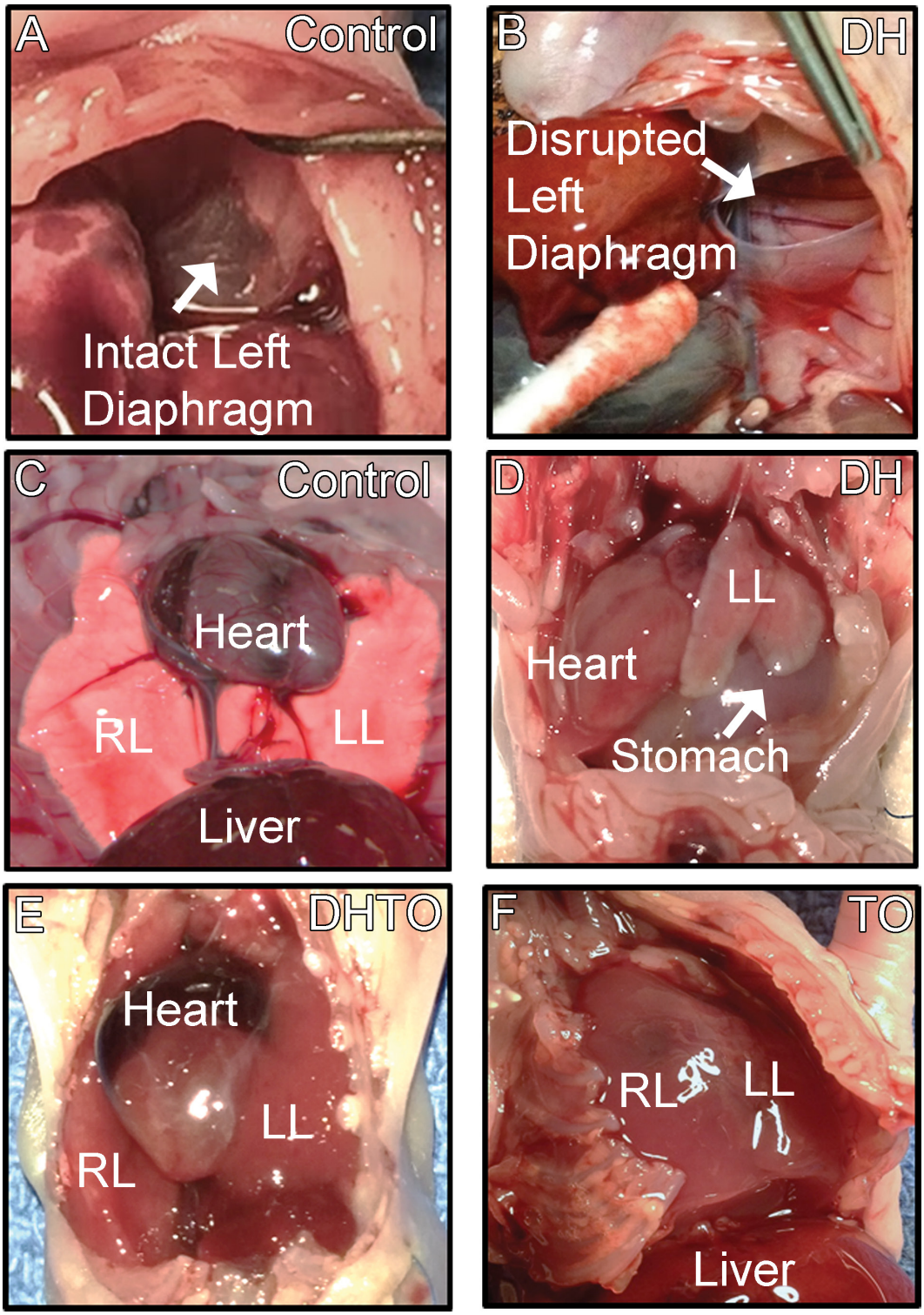

Figure 2. Surgical Model of CDH and CDH/TO. (A) The intact left diaphragm of an E30.5 rabbit fetus. (B) The disrupted left diaphragm of a diaphragmatic hernia (DH) fetus. (C) Normal size of the right lung (RL) and left lung (LL) in a control E30.5 rabbit fetus. (D) Herniation of abdominal contents into the left chest in DH resulted in lung hypoplasia and displacement of thoracic organs to the right. (E) Tracheal occlusion (TO) after DH increased lung size, resolved the rightward shift and reduced herniation of abdominal contents into the thorax. (G) TO alone increased lung size beyond that of control.

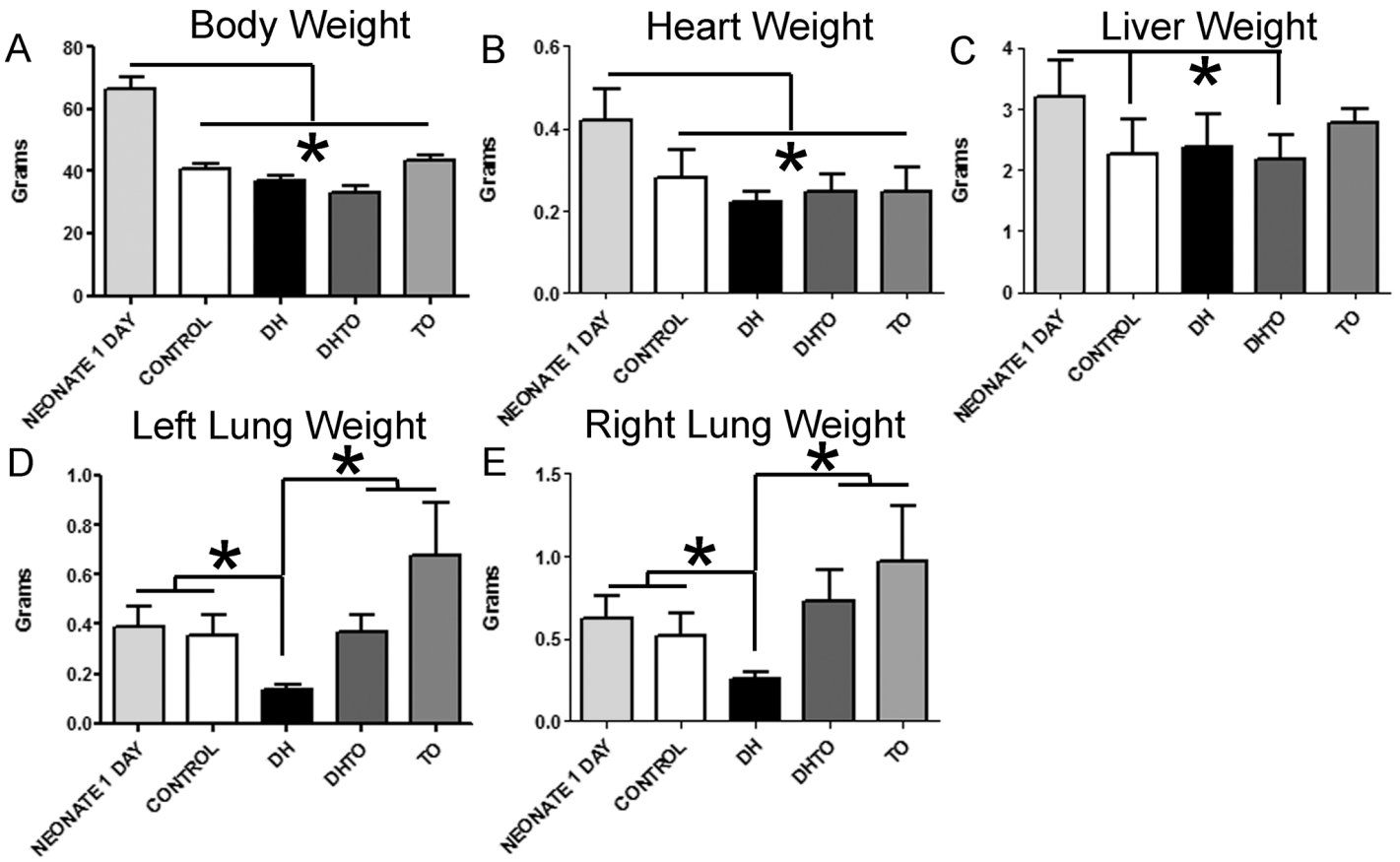

Figure 3. Organ and body weights in DH and DHTO. (A) DH and TO surgeries did not result in any significant difference in fetal body weight, (B) fetal heart weight, or (C) fetal liver weight. (D) DH resulted in a decrease in left lung weight compared with all other groups. TO alone resulted in a left lung that was larger than all other groups (not shown for clarity purposes). (E) DH induced similar changes in the right lung as the left. Right lung weight in TO alone was significantly greater than d 1, control and DH lung (not shown for clarity purposes).

Comparison to Other Published Gene Expression Datasets

We compared our gene expression data set to a recently published a gene expression dataset using a similar fetal rabbit surgical model (17). Of the 641 differentially expressed genes reported by Engels, *et al*. across all groups, 500 were also differentially expressed in our data sets. In evaluating similarities and differences in group to group comparisons between studies, there was a high degree of correlation between patterns of gene expression between DH and DHTO ($p = 9.3 \times 10^{-19}$); however, gene expression between control and DH was weakly anticorrelated ($OR = 0.46$, $p = 0.0003$). Agreement between our dataset and a previously published one is high in comparing DHTO to DH but low in comparing DH to control.

TO Reverses and Overcompensates for DH Lung Gene Expression Changes

We used hierarchical clustering to determine whether DH induced significant changes in gene expression compared with control and the impact of TO on these changes. After false discovery rate correction using a generous significance threshold of $p < 0.1$, there were fewer than ten genes that were differentially expressed in DH or DHTO compared with control, but 687 in DHTO compared with DH (Figure 4A). Examination of the gene expression heat map revealed that many of the genes downregulated by DH were upregulated to an even greater degree by DHTO compared with control. By hierarchical clustering, DHTO was more different from DH than control and one TO gene expression profile was most similar to control and the other was most similar to DHTO (Figure 4B). We used Gene Expression Dynamic Inspector (GEDI) heat maps of the average gene expression of each group to better visualize these differences (25). Although there were many similarities, DHTO had higher expression of one set of genes (region 1) and lower expression of another set of genes (region 2) than control, DH, or TO. A third set of genes (region 3) were downregulated in DH and increased in DHTO to a level greater than that of control (Figure 4C). These data indicate that in this rabbit model of DH with

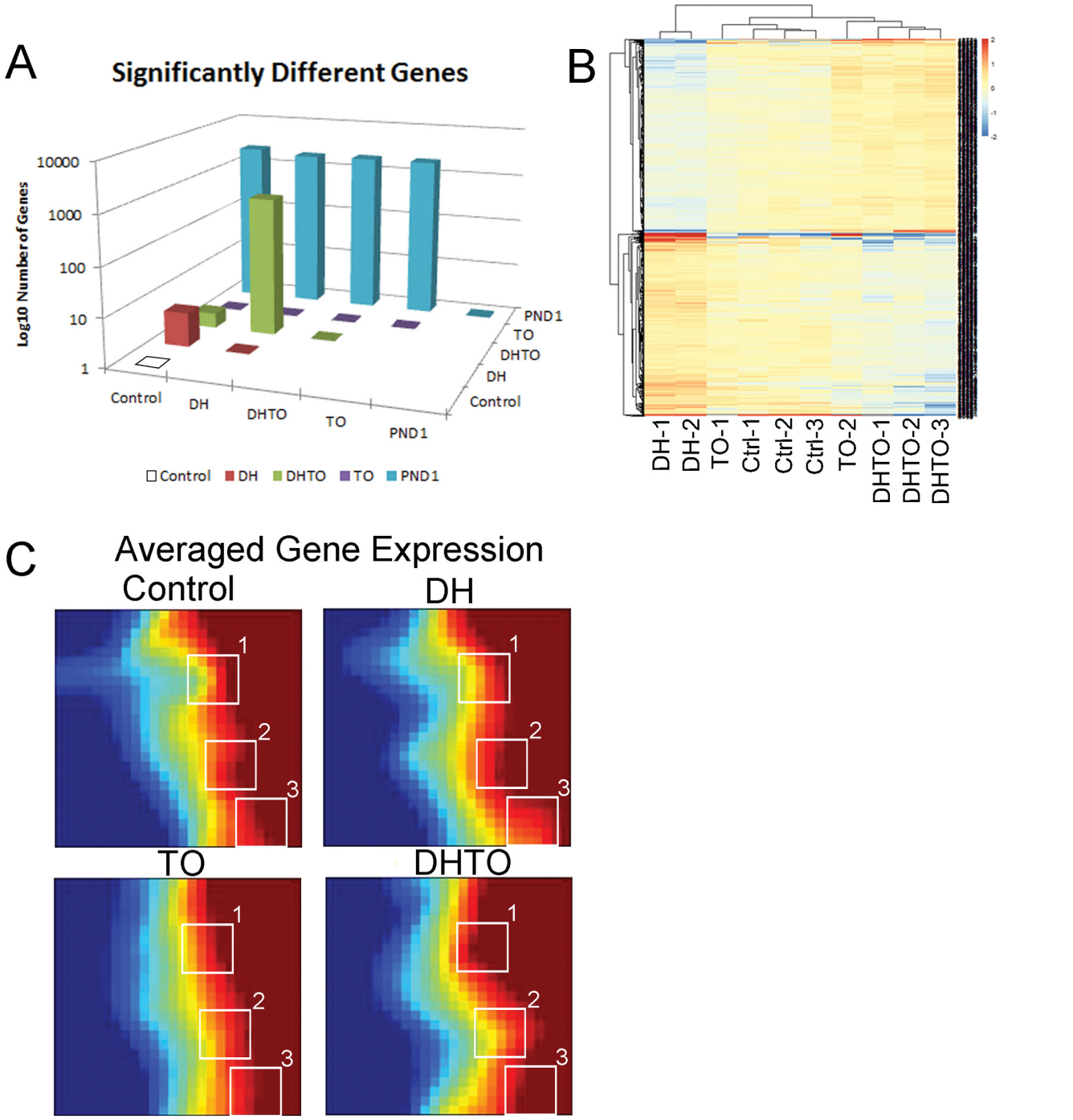

Figure 4. TO reverses and overcompensates for many of the gene expression changes induced by surgical DH. (A) After false discovery correction and using a $p < 0.1$ level of significance and comparing each group to the others, there were very few genes with significantly different levels of expression among the 13,687 genes analyzed. The exception to this was an increased number of differentially expressed genes between DH and DHTO (687 genes). As expected, PND1 rabbit lung had more differentially expressed genes than fetal lung time points. Note the log10 scale. (B) Hierarchical clustering of gene expression profiles demonstrated that TO was more similar to control than DHTO and that DHTO was more like control (Ctrl) than DH. (C) Gene Expression Dynamics Inspector (GEDI) was used to generate average gene expression heat maps for each fetal lung group. DHTO had higher expression of the genes grouped in region 1 and lower levels of gene expression in region 2 compared with control, DH and TO. In region 3, DH had reduce levels of gene expression compared with control and DHTO had higher expression levels of these genes.

and without TO, TO reverses and overcompensates for many of the lung gene expression changes induced by DH and that the DHTO gene expression profile is distinct from that of control, DH and TO alone.

The Immature Lung Phenotype Induced by DH Is Not Reversed by TO

Since the number of genes differentially expressed was greater in DHTO compared with control or DH, we hypothesized that genes expressed in earlier lung development were being persistently expressed in DH and that TO would restore these genes to a more normal developmental gene expression profile. To test this hypothesis, we quantified the correlation of our rabbit lung whole lung gene expression data set to a published mouse lung development gene expression dataset (24). Both DH and DHTO lungs demonstrated increased expression of genes expressed in the mouse lung between E12 and E16 with no differences between the groups with genes expressed at later time points (Figure 5A). We used GEDI heat maps to visually compare lung gene expression profiles between mouse and rabbit fetus. Of the three areas of gene expression identified as different between DHTO and control and DH, normal lung development was associated with downregulation of one set of genes that were upregulated in DHTO compared with control (region 1), but lung maturation was also associated with upregulation of another set of genes that were also upregulated in DHTO (region 3) (Figure 5B). The effect of TO on DH lung gene expression profile is mixed, but overall TO does not alter the immature lung gene expression profile of DH lung.

TO after DH Increases DNA Replication and Epithelial Cell Proliferation

To understand the differentially regulated genes in DH and DHTO, the unique and common genes for each condition were identified and subjected to pathway analysis (Figure 6A) (31). Fifty-four or fewer genes were unique to DH, control, DH + control, or DH + DHTO. Three hundred ninety-seven genes were unique to DHTO and 369 genes were unique to DHTO + control. Pathway analysis of the genes unique to DHTO and comparing them to DH demonstrated that DNA synthesis and DNA elongation were the only upregulated processes (Figure 6B) (32,33). We validated these findings by quantifying epithelial cell proliferation in fetal rabbit lung sections. Tile scanned images of fetal rabbit lungs were stained for the cell proliferation marker phosphohistone 3 (pH3) and the epithelial transcription factor thyroid transcription factor-1 (TTF1, Nkx-2.1) and percentage of nuclei positive for one or both markers was quantified (Figure 6C,D). The frequency of pH3-positive nuclei in DH was half that of control, and the frequency in DHTO was 2.3-fold higher than DH. pH3-positive nuclei were 20% higher in TO compared with DHTO (Figure 6E, ANOVA $p = 0.07$). These differences were even more marked in epithelial cells (Figure 6F, ANOVA $p = 0.02$). These bioinformatic and cell proliferation data indicate that DH suppresses lung cell proliferation—particularly epithelial cell proliferation—and TO reverses and overcompensates for this reduction.

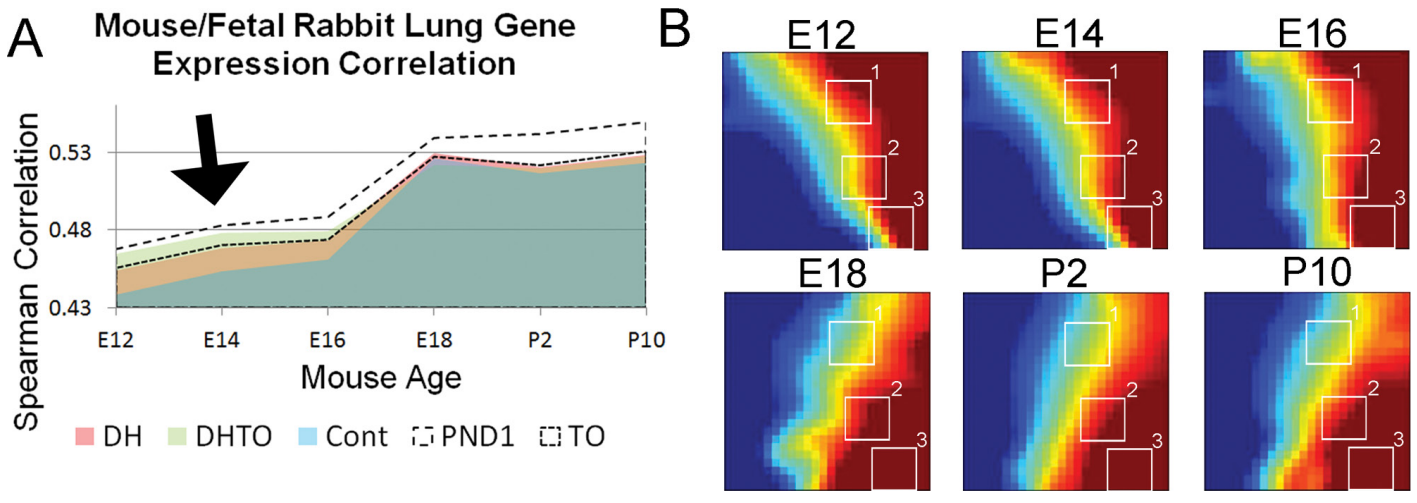

Figure 5. TO does not reverse the immature lung gene expression profile induced by DH. (A) Rabbit lung gene expression was correlated to that of published mouse lung development data (24). While there was a high degree of correlation at E18 and beyond, DHTO and DH lung were more highly correlated at E12, E14 and E16 than control lung. The colors used in this panel are translucent with olive indicating DH, TO and DHTO and orange DH and DHTO. (B) The average gene expression profile of each mouse lung age was plotted on the same matrix as the previous fetal rabbit lung matrix. Over the course of lung development, gene expression in region 1 decreases and gene expression in region 3 increases. Gene expression in region 2 is overall unchanged although the pattern changes.

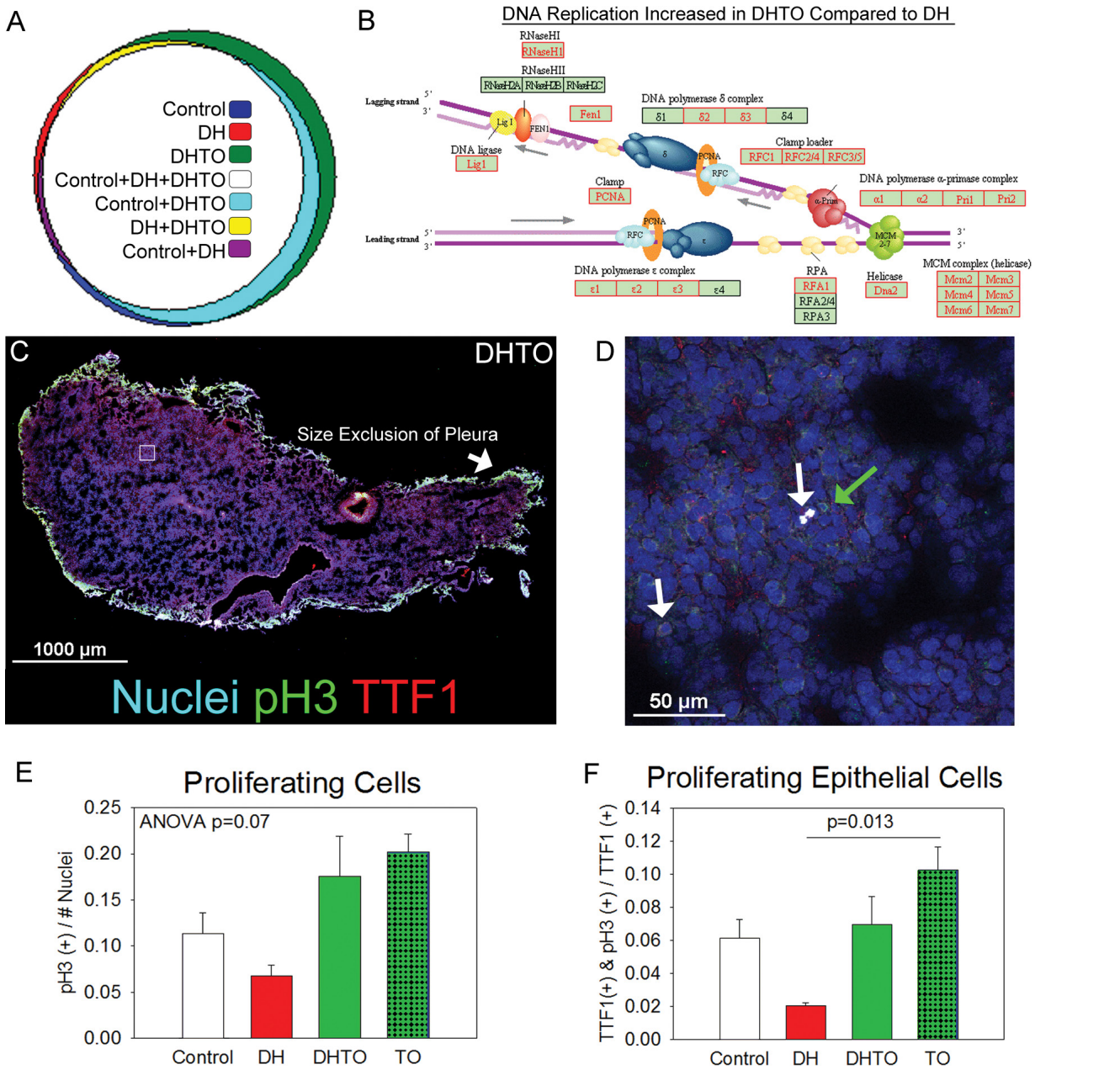

Figure 6. TO after DH increases DNA replication and cell division. (A) Among the 13,687 profiled genes, very few were uniquely expressed in control, DH, DH + control, or DH + DHTO. The majority of unique genes were expressed in DHTO (397) with a similar number in DHTO + Control (369). A proportionate Venn diagram was created using a web app from the Massachusetts Institute of Technology (31). (B) The only processes upregulated in DHTO compared with DH were DNA replication and elongation. Superimposing this gene expression profile onto the KEGG pathway for DNA replication demonstrate that expression of each component of the DNA replication complex is increased in DHTO (32,33). Red lettering indicates genes with increased expression levels. (C) Control, DH, DHTO and TO lung sections (n = 6–12) stained for the cell proliferation marker phospho-histone 3 (pH3, green) and thyroid transcription factor 1 (TTF1, Nkx-2.1, red) were imaged by tile scan and nuclear (blue) co-localization of pH3 and TTF1 quantified. The autofluorescent pleural surface was excluded by object size filtering. (D) Confocal imaging of a region of the prior image demonstrated nuclei expressing both markers (white arrows) and only pH3 (green arrow). In this representative image only strongly positive cells are highlighted. (E) Quantification of total number of pH3-positive nuclei demonstrated a 2-fold reduction in DH compared with control and a 3-fold increase in DHTO and TO compared with DH. (F) Limiting analysis to TTF1-positive cells, there was a 3-fold reduction in pH3-positive epithelial cells in DH compared with control with a 3.4-fold increase in DHTO compared with DH and an additional 47% increase in TO compared with DHTO.

DH Increases Ribosomal Biogenesis which is Reversed by TO

Analyzing the genes downregulated in DHTO compared with DH, the significantly impacted processes were signal recognition particle (SRP)-dependent co-translational protein targeting to membrane, translation termination, co-translational protein targeting to membrane, protein targeting to ER, and establishment of protein localization to endoplasmic reticulum. Ribosomal biogenesis was the only pathway downregulated in DHTO compared with DH (Figure 7). Despite these bioinformatic findings, there was no difference in 18S RNA content in control, DH, DHTO, or DH lung. These data suggest that the DH lung persists in a state of high protein synthesis which is reversed by TO.

Reciprocal Regulation of Protein Synthesis Pathways, Epidermal Growth Factor Receptor, and Ephrin Signaling in DHTO and CDH

Since the gene expression profiles reversed by TO after DH were not strictly related to lung development *per se*, we compared reciprocally upregulated genes in DH and DHTO to understand the impact of each on lung development.

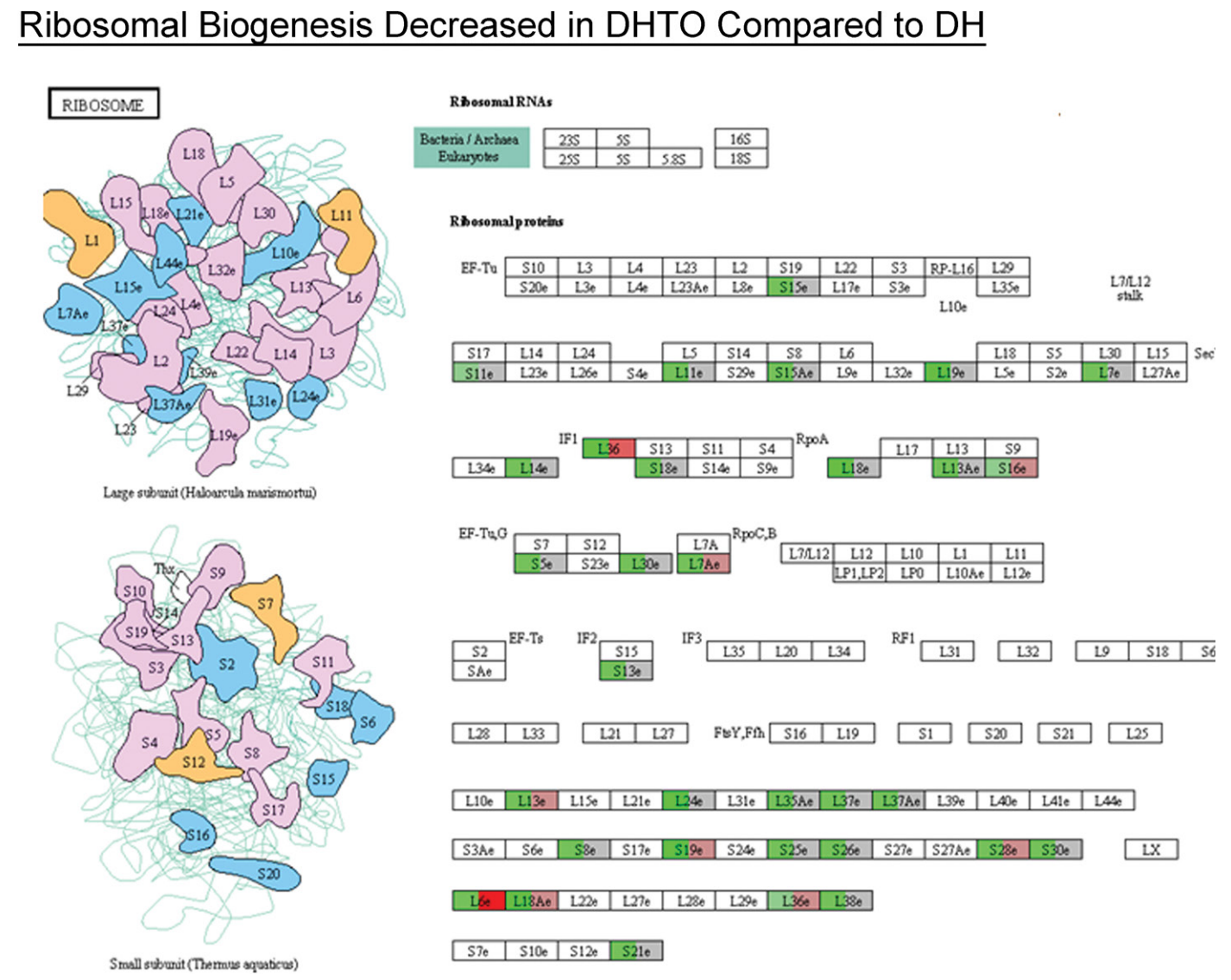

Figure 7. TO reverses increased protein synthesis pathways in the DH lung. The processes downregulated in DHTO compared with DH involved protein synthesis, protein trafficking and ribosomal biogenesis. The ribosomal biogenesis KEGG pathway demonstrates reduced expression of many ribosomal genes in DHTO / DH (32,33). Differentially expressed genes are colored, with the left half color indicating expression change in DHTO versus Control, and right half DH versus control. Red boxes indicate upregulated genes, green boxes downregulated genes, and gray boxes expressed genes without different mRNA levels. White boxes indicate genes that did not meet our inclusion criteria.

Consistent with our gene expression findings (Figure 4), the pathways and processes downregulated by DH were excessively upregulated in DHTO and vice versa (Figure 8A). The five most significant processes downregulated in DH and upregulated by DHTO were axon development, epidermal growth factor receptor (EGFR) signaling, hydroxylase activity, axonogenesis and EGFR-B (ErbB) signaling. The most significant signaling pathways were phosphatidylinositol signaling and Jak-STAT signaling. Conversely, the five processes most significantly upregulated by DH and downregulated in DHTO were signal recognition particle (SRP)-dependent co-translational protein targeting to membrane, translation termination, co-translational protein targeting to membrane, protein targeting to ER and establishment of protein localization to endoplasmic reticulum. The process most significantly upregulated by DH and downregulated by DHTO involved ribosome biogenesis (Figure 8B). In comparing the percentage of downregulated genes in DHTO compared with DH and the percentage upregulated in DH compared with control, all of the top ten pathways demonstrated a reciprocal relationship although the downregulation in DHTO/DH was greater than the upregulation of DH/Control (Figure 8C). Similarly, the genes upregulated in DHTO/DH were reciprocally downregulated in DH/Control (Figure 8D). Similar to the list of top regulated processes when all groups were considered, EGFR and ephrin signaling were represented; however, unlike the prior list, two of the top three processes were related to cell migration and small GTPase activity. These data demonstrate that TO reverses many of the gene regulator changes induced by DH, but in most of these processes the level of reversal exceeds levels seen in control.

DISCUSSION

Using a rabbit surgical model of CDH and TO, we demonstrated that TO reverses some of the gene expression changes induced by CDH and that TO reverses increased protein biosynthetic and reduced cell proliferation activity in CDH lung. However, the reversal of these genes and pathways exceeds gene expression and pathway activity levels of control lung. Many of these findings can be explained by increased EGFR and ephrin signaling in DHTO lung. By comparing DH and DHTO gene expression profiles to that seen over the course of normal lung development, both DH and DHTO lungs were more immature than age-matched control fetal rabbit lung. Due to the small number of differentially regulated genes in TO alone, we could not define any pathways regulated by cyclic versus static stretch. Since ongoing phase I trials are testing the feasibility of using TO to improve lung health in human CDH (5), these findings provide insight into how this fetal surgical therapy alters cellular signaling and processes and identifying targets which may further improve lung health in this devastating condition.

DHTO upregulated DNA synthesis pathways and cell division and decreased ribosomal pathways when compared with DH. While it may at first seem counterintuitive that these two processes would not be coupled, this divergent relationship could perhaps be understood as the divergence between cellular hypertrophy and hyperplasia. Conceptually, increasing airspace size requires a larger number of cells to line this airspace, and in the absence of airspace enlargement, cell division is retarded and cell energy is diverted to cell growth. In our study, DHTO lungs demonstrated decreased protein synthesis compared with DH and control lungs, although no specific protein group, such as surfactant proteins, were differentially regulated. This is consistent with human studies demonstrating no difference in surfactant quality or composition in CDH (13) but is inconsistent with animal studies showing the opposite (10,11). With regards to cell hyperplasia, using nitrofen model of CDH, Chapin, *et al*. demonstrated that rat DH lungs contain less DNA than control and that lung DNA content is increased by TO (10). Saada, *et al*. observed epithelial hyperplasia in a sheep model of DHTO (11), and after TO in the rat nitrogen model, there is an increased ratio of alveolar type I to alveolar type II cells (10). Taken together, these findings suggest than one or more epithelial mitogens may be important in the adaptive and maladaptive responses in CDH treated with TO.

We found that EGFR and ephrin signaling were reduced in DH and excessively increased in DHTO. EGFR signaling is central to the development of many nonsmall cell lung carcinomas and is a common chemotherapeutic target (34). When lung carcinomas escape EGFR regulation, they do so by enhanced ephrin signaling, and new chemotherapeutics are now in development targeting both EGFR and ephrin signaling (35). EGFR is critical for alveolar type II cell self-renewal (36) and is important for myofibroblast migration during alveolar septation (37). Excessive pulmonary EGFR signaling in mice arrests lungs in the saccular stage of lung development with poor epithelial-endothelial apposition and death by P7 (38). Disruption of ephrin signaling has similar consequences for lung development with failed septation (8) and hypoplasia of the pulmonary microvasculature (14). Both EGFR and ephrin receptors are receptor tyrosine kinase and signal via phosphatidylinositol and Jak-STAT signaling—both pathways that were downregulated in DH and upregulated in DHTO in our data set. Our findings regarding EGFR and ephrin signaling potentially explain many of the disruptions of epithelial function and lung morphogenesis in CDH and CDHTO.

Consistent with the findings of other groups (6), one of the top regulated pathways in DHTO involved cell migration and lamellipodium formation via *CDC42* and *Rac1*. This signaling may be related to EGFR as it acts both via Csk/Src and *RhoA* (another small GTPase) to regulated myofibroblast migration during alveolar development (37); however these pathways are activated in response

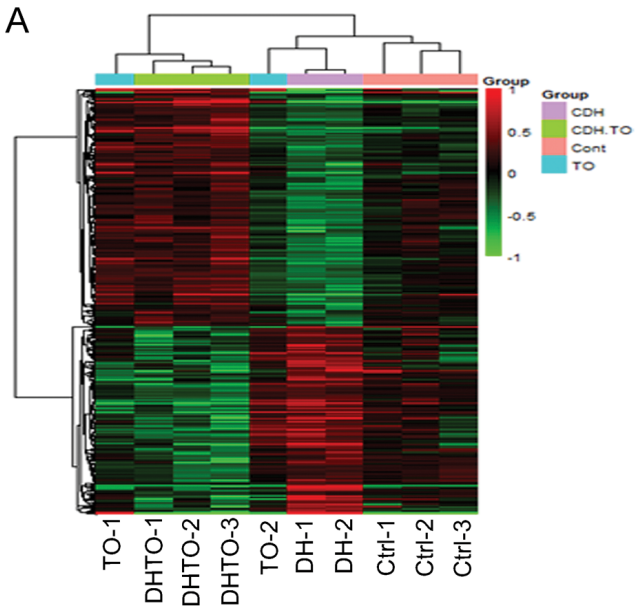

B

Downregulated in DH & Reversed in DHTO

Category	CategoryID	CategoryDescription	nDE	nTotal	FisherFDR	logOR
GO.BP	GO:0061564	axon development	27	427	9.29E-02	0.997
GO.BP	GO:0007173	epidermal growth factor receptor signaling pathway	15	176	9.29E-02	1.32
GO.BP	GO:0051345	positive regulation of hydrolase activity	34	636	9.29E-02	0.82
GO.BP	GO:0007409	axonogenesis	25	410	9.29E-02	0.954
GO.BP	GO:0038127	ERBB signaling pathway	15	181	9.29E-02	1.289
KEGG	hsa04070	Phosphatidylinositol signaling system	7	59	1.20E-01	1.709
KEGG	hsa00562	Inositol phosphate metabolism	6	46	1.20E-01	1.826
KEGG	hsa04630	Jak-STAT signaling pathway	8	82	1.20E-01	1.484
GO.BP	GO:0048675	axon extension	8	60	1.41E-01	1.846
GO.BP	GO:0042059	negative regulation of epidermal growth factor receptor signaling pathway	6	34	1.46E-01	2.192

Upregulated in DH & Reversed in DHTO

Category	CategoryID	CategoryDescription	nDE	nTotal	FisherFDR	logOR
KEGG	hsa03010	Ribosome	32	61	2.66E-35	4.167
GO.BP	GO:0006614	SRP-dependent cotranslational protein targeting to membrane	31	80	1.06E-29	3.657
GO.BP	GO:0006415	translational termination	37	136	1.06E-29	3.169
GO.BP	GO:0006613	cotranslational protein targeting to membrane	31	82	1.19E-29	3.617
GO.BP	GO:0045047	protein targeting to ER	31	84	2.19E-29	3.579
GO.BP	GO:0072599	establishment of protein localization to endoplasmic reticulum	31	86	4.17E-29	3.543
GO.BP	GO:0000184	nuclear-transcribed mRNA catabolic process, nonsense-mediated decay	31	87	5.31E-29	3.525
GO.BP	GO:0006414	translational elongation	37	156	7.58E-28	2.984
GO.BP	GO:0070972	protein localization to endoplasmic reticulum	32	105	1.26E-27	3.299
GO.MF	GO:0003735	structural constituent of ribosome	33	108	3.55E-27	3.213
GO.BP	GO:0019083	viral transcription	34	146	3.43E-25	2.943
GO.BP	GO:0006413	translational initiation	38	199	4.46E-25	2.712
GO.BP	GO:0019080	viral gene expression	34	154	1.92E-24	2.874
GO.BP	GO:0044033	multi-organism metabolic process	34	160	6.90E-24	2.825
GO.BP	GO:0006612	protein targeting to membrane	32	139	1.47E-23	2.918

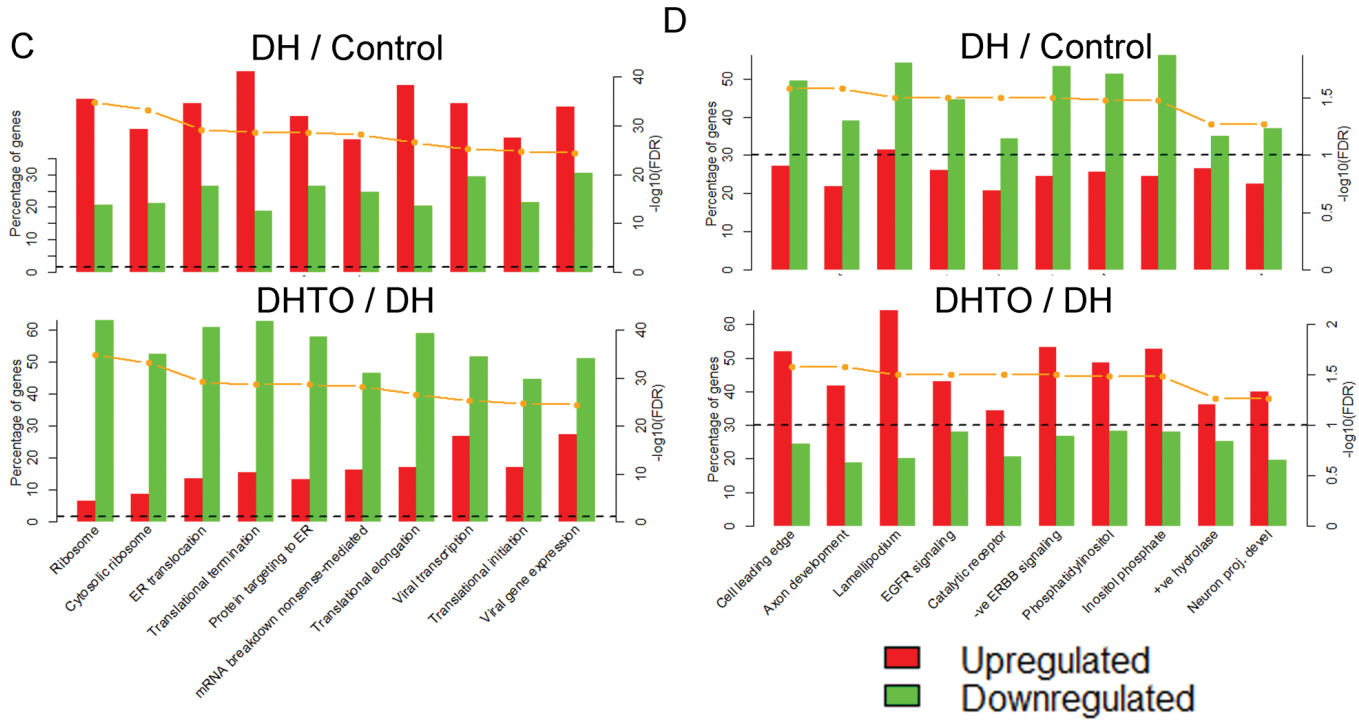

Figure 8. Reciprocal gene regulatory patterns in DH and DHTO. (A) Hierarchical clustering of genes increased in DHTO and decreased in DH yielded clusters similar to clustering using all genes except that in this analysis one TO sample was most similar to DHTO and one TO sample was most similar to DH. The expression of genes in the control group was generally between that of DHTO and DH. (B) Pathway analysis of genes downregulated in DH and upregulated in DHTO revealed that the top ten upregulated pathways and processes were all downstream of epidermal growth factor receptor or ephrin signaling. The top fifteen pathways downregulated in DH and upregulated in DHTO all involved protein synthesis or trafficking. (C) The ten most significantly altered processes downregulated in DHTO versus DH all involved protein synthesis or trafficking and had reciprocal upregulation in DH versus control. The dashed line represents statistical significance. (D) The top ten upregulated processes in DHTO versus DH also had reciprocal downregulation in DH versus control. Similar to the list of top regulated processes using differentially regulated genes in all groups, epidermal growth factor receptor and ephrin signaling (axon development) were represented, but two of the top three processes involved small GTPases (cell leading edge and lamellipodium).

to cellular strain and are necessary for cell spreading; so, it seems most likely that these small GTPases are principally activated by the mechanical stimulus of future airspace enlargement.

Could pharmacologic manipulation of small GTPases, ephrin signaling, or EGFR signaling improve lung function after TO for CDH, and could these therapies be selectively targeted to the lung? The goal of such therapy would be to prevent epithelial hyperplasia, promote epithelial maturity and improve lung function after TO for CDH. Previous work has demonstrated the feasibility of administering compounds tracheally at the time of tracheal occlusion and that large proteins (such as vascular endothelial growth factor (VEGF)-164) impact nonepithelial lung structure and function (15). It seems likely that small molecule inhibitors would have systemic absorption and probably undesirable nonpulmonary effects. Furthermore, small GTPase inhibition is likely undesirable due to its role in epithelial spreading. There are two therapeutic approaches to inhibiting EGFR and ephrin signaling. The first is to inhibit the tyrosine kinase activity of one or both receptors, and the second is to use a monoclonal antibody to inactivate the ligand or receptor (34,35). While additional work needs to be done identifying the key ligand or ligands, this second approach could be used to attenuate EGFR and/or ephrin signaling which could improve lung maturity and function and ultimately reduce mortality in infants with CDH treated with TO.

Our findings largely complement other published findings using a similar fetal rabbit surgical model. In a recent publication, Engels, *et al*. performed DH surgery two days earlier (d 23) and TO one day later (d 28) than in our study. His group reported that DHTO is associated with increased expression of genes associated with cell proliferation, and examination of expression data revealed that many genes with increased and decreased expression in DH are reversed in DHTO to expression levels exceeding that of control (17). We found many fewer significantly different genes in DH versus control than Engels, *et al*. but comparable numbers in DHTO versus DH. Since we created the DH at a later time point and observed a lesser difference in gene expression in that group compared with control, the difference in findings are likely due to differences in lung maturity at the time of DH. The similar number of differentially expressed genes in DHTO versus DH despite a three day difference in the time between DH and DHTO suggest that these gene expression changes are biomechanically regulated and not part of a conserved, stereotyped lung morphogenetic program.

We did not find significant alterations in pathways regulating synthesis of extracellular matrix. Vukovich, *et al*. reported both elastogenesis and transforming growth factor-β signaling were increased in DHTO to levels beyond those of DH or control (6,7). Again, our findings regarding these processes did not reach statistical significance; however their findings are consistent with the observed pattern that processes impacted by DH are excessively reversed in DHTO.

The reader should consider several mitigating factors in evaluating our study. (1) We assumed that position in the uterine horn did not affect lung gene expression. We did not randomly assign fetuses to treatment group so as not to be confused as to group in the event of fetal demise. (2) We cannot draw strong conclusions on the effect of TO alone on lung gene expression since one fetus had a gene expression profile most similar to control and one had a profile most like DHTO. (3) Congenital diaphragmatic hernia results in displacement of abdominal contents at an earlier time point than the surgical DH model. Chemical models of diaphragmatic hernia more closely mimic the natural history of CDH, but they unfortunately rely on antagonism of retinoic acid signaling which is crucial to normal lung development (39). A recent study comparing human CDH, surgical rabbit DH and rat nitrofen DH indicated that human and rabbit lungs demonstrated upregulation of the vitamin A metabolic program supporting the view that surgical DH more closely mimics human CDH (40). (4) The rabbit genome is not as well annotated as is the mouse, rat, or human genomes and thus some genes may have been missed in our analysis. (6) Similarly, there is no available dataset profiling rabbit lung gene expression over the course of development. While comparison to mouse lung development is informative, such analysis is limited by differences between the species. (7) Lastly, our DH model uses a left diaphragm defect and we analyzed the lateral aspect of the left upper lobe. While other investigators have shown similar gene expression profiles in left and right lungs after left or right DH (7,9,10), one paper did report differences in surfactant gene expression between right and left lungs (12). We did not perform validation experiments comparing right and left lungs.

CONCLUSION

We have demonstrated that DH induces a persistently immature lung gene expression profile and that TO does not significantly reverse this profile. TO does however reverse alterations in ephrin, EGFR, cell proliferation and protein biosynthetic pathways. These findings elucidate the most significantly regulated processes and pathways in DH and DHTO and identify targets for future CDH therapies.

ACKNOWLEDGMENTS

We would like to acknowledge Jordan Wolfe for helping to inspire this project and Jeffrey Whitsett for providing mentorship during its development.

DISCLOSURES

Funding was provided by the Parker B. Francis Family Foundation (BMV); the Procter Scholar Program at CCHMC (BMV); the National Council of Technological and Scientific Development (CNPq) #302433/2014-7 (LS) and #233775/2014-5 (RLF); and the Sao Paulo Research Foundation (Fapesp) #2014/02519-6 (LS).

REFERENCES

1. Coughlin MA, *et al*. (2015) Prenatally diagnosed severe CDH: mortality and morbidity remain high. *J. Pediatr. Surg*. [Epub ahead of print 2015 Nov 10].
2. Paris ND, Coles GL, Ackerman KG. (2015) Wt1 and beta-catenin cooperatively regulate diaphragm development in the mouse. *Dev. Biol*. 407:40–56.
3. Jani JC. *et al*. (2009) Severe diaphragmatic hernia treated by fetal endoscopic tracheal occlusion. *Ultrasound Obstet. Gynecol*. 34:304–10.
4. Deprest J, Gratacos E, Nicolaides KH; FETO Task Group. (2004) Fetoscopic tracheal occlusion (FETO) for severe congenital diaphragmatic hernia: evolution of a technique and preliminary results. *Ultrasound Obstet. Gynecol*. 24:121–6.
5. Al-Maary J. *et al*. (2016) Fetal tracheal occlusion for severe pulmonary hypoplasia in isolated congenital diaphragmatic hernia: a systematic review and meta-analysis of survival. *Ann. Surg*. [Epub ahead of print 2016 Feb 22].
6. Vuckovic A, *et al*. (2016) Increased TGF-beta: a drawback of tracheal occlusion in human and experimental congenital diaphragmatic hernia? *Am. J. Physiol. Lung Cell. Mol. Physiol*. 310:L311–L327.
7. Vuckovic A, *et al*. (2012) Signaling molecules in the fetal rabbit model for congenital diaphragmatic hernia. *Pediatr. Pulmonol*. 47:1088–96.
8. Wilkinson GA, *et al*. (2008) Role for ephrinB2 in postnatal lung alveolar development and elastic matrix integrity. *Dev. Dyn*. 237:2220–34.
9. Boucherat O, *et al*. (2007) Decreased lung fibroblast growth factor 18 and elastin in human congenital diaphragmatic hernia and animal models. *Am. J. Respir. Crit. Care Med*. 175:1066–77.
10. Chapin CJ, *et al*. (2005) Congenital diaphragmatic hernia, tracheal occlusion, thyroid transcription factor-1, and fetal pulmonary epithelial maturation. *Am. J. Physiol. Lung Cell. Mol. Physiol*. 289:L44–L52.
11. Saada J, *et al*. (2010) Combining keratinocyte growth factor transfection into the airways and tracheal occlusion in a fetal sheep model of congenital diaphragmatic hernia. *J. Gene Med*. 12:413–22.
12. Davey MG, *et al*. (2005) Surfactant protein expression is increased in the ipsilateral but not contralateral lungs of fetal sheep with left-sided diaphragmatic hernia. *Pediatr. Pulmonol*. 39:359–67.
13. Boucherat O, *et al*. (2007) Surfactant maturation is not delayed in human fetuses with diaphragmatic hernia. *PLoS Med*. 4:e237.
14. Vadivel A, *et al*. (2012) Critical role of the axonal guidance cue EphrinB2 in lung growth, angiogenesis, and repair. *Am. J. Respir. Crit. Care Med*. 185:564–74.
15. Debeer A, *et al*. (2010) Antenatal fetal VEGF therapy to promote pulmonary maturation in a preterm rabbit model. *Early Hum. Dev*. 86:99–105.
16. Makanga M, *et al*. (2013) Downregulated bone morphogenetic protein signaling in nitrofen-induced congenital diaphragmatic hernia. *Pediatr. Surg. Int*. 29:823–34.
17. Engels AC, *et al*. (2016) Pulmonary transcriptome analysis in the surgically induced rabbit model of diaphragmatic hernia treated with fetal tracheal occlusion. *Dis. Model. Mech*. 9:221–8.
18. Fauza DO, *et al*. (1994) Surgically produced congenital diaphragmatic hernia in fetal rabbits. *J. Pediatr. Surg*. 29:882–6.
19. Ritchie ME, *et al*. (2015) limma powers differential expression analyses for RNA-sequencing and microarray studies. *Nucleic Acids Res*. 43:e47.
20. Law CW, *et al*. (2014) voom: precision weights unlock linear model analysis tools for RNA-seq read counts. *Genome Biol*. 15:R29.
21. Craig, D.B., S. Kannan, and A.A. Dombkowski. (2012) Augmented annotation and orthologue analysis for *Oryctolagus cuniculus*: Better Bunny. *BMC Bioinformatics*. 13:84.
22. Freudenberg JM, *et al*. (2009) CLEAN: CLustering Enrichment ANalysis. *BMC Bioinformatics*. 10:234.
23. Luo W, Brouwer C. (2013) Pathview: an R/Bioconductor package for pathway-based data integration and visualization. *Bioinformatics*. 29:1830–1.
24. Dong J, *et al*. (2010) MicroRNA networks in mouse lung organogenesis. *PLoS One*. 5:e10854.
25. Eichler GS, Huang S, Ingber DE. (2003) Gene Expression Dynamics Inspector (GEDI): for integrative analysis of expression profiles. *Bioinformatics*. 19:2321–2.
26. Kho AT, *et al*. (2009) Expression profiles of the mouse lung identify a molecular signature of time-to-birth. *Am. J. Respir. Cell Mol. Biol*. 40:47–57.
27. Bult CJ, *et al*. (2016) Mouse genome database 2016. *Nucleic Acids Res*. 44(D1):D840–D847.
28. Pringle KC. (1986) Human fetal lung development and related animal models. *Clin. Obstet. Gynecol*. 29:502–13.
29. Roubliova X, *et al*. (2004) Pulmonary vascular morphology in a fetal rabbit model for congenital diaphragmatic hernia. *J. Pediatr. Surg*. 39: 1066–72.
30. Toelen J, *et al*. (2011) The fetal respiratory system as target for antenatal therapy. *Facts Views Vis. Obgyn*. 3:22–35.
31. Bioinformatics and Research Computing. *3 Way Venn Diagram Generator*. 2012 August 16, 2012 [accessed 2016 March 16]; Program for Creating Proportionate Venn Diagrams. http://jura.wi.mit.edu/bioc/tools/venn3way/index.php.
32. Kanehisa M, *et al*. (2016) KEGG as a reference resource for gene and protein annotation. *Nucleic Acids Res*. 44(D1):D457–D462.
33. Ogata H, *et al*. (1999) KEGG: Kyoto Encyclopedia of Genes and Genomes. *Nucleic Acids Res*. 27:29–34.
34. Han W, Lo HW. (2012) Landscape of EGFR signaling network in human cancers: biology and therapeutic response in relation to receptor subcellular locations. *Cancer Lett*. 318:124–34.
35. Giaccone G, Wang Y. (2011) Strategies for overcoming resistance to EGFR family tyrosine kinase inhibitors. *Cancer. Treat. Rev*. 37:456–64.
36. Desai TJ, Brownfield DG, Krasnow MA. (2014) Alveolar progenitor and stem cells in lung development, renewal and cancer. *Nature*. 507:190–4.
37. Li J, *et al*. (2016) Csk/Src/EGFR Signaling regulates migration of myofibroblasts and alveolarization. *Am. J. Physiol. Lung Cell. Mol. Physiol*. 310:L562–L71.
38. Kramer EL, *et al*. (2007) Perinatal increases in TGF-{alpha} disrupt the saccular phase of lung morphogenesis and cause remodeling: microarray analysis. *Am. J. Physiol. Lung Cell. Mol. Physiol*. 293:L314–L27.
39. Keijzer R, *et al*. (2000) Dual-hit hypothesis explains pulmonary hypoplasia in the nitrofen model of congenital diaphragmatic hernia. *Am. J. Pathol*. 156:1299–1306.
40. Coste K, *et al*. (2015) Metabolic disturbances of the vitamin A pathway in human diaphragmatic hernia. *Am. J. Physiol. Lung Cell. Mol. Physiol*. 308:L147–L157.

Cite this article as: Varisco BM, *et al*. (2016) Excessive reversal of epidermal growth factor receptor and ephrin signaling following tracheal occlusion in rabbit model of congenital diaphragmatic hernia. *Mol. Med*. 22:398–411.